

EXPERIMENT AND RESEARCH ON PREDICTED MODEL OF FOREST FIRE SPREAD BASED ON ENSEMBLE KALMAN FILTER

S. ZHANG¹, J. LIU¹, H. GAO¹, X. CHEN¹, X. LI^{1,2*}, J. HUA¹, H. HU³

¹ College of Mechanical and Electrical Engineering, Northeast Forestry University, Harbin 150040, China;

² Northern Forest Fire Management Key Laboratory of the State Forestry and Grassland Bureau, Northeast Forestry University, Harbin 150040, China

³ College of Forestry, Northeast Forestry University, Harbin 150040, China

*Corresponding Author

ABSTRACT. The spread of forest fire is an extremely complex and harmful natural phenomenon. The existing model fails to combine the influence factors of forest fire spread, and the the error of prediction will increase with time. In this paper, the Ensemble Kalman Filter (ENKF) algorithm is applied to the field of forest fire spread so that it can better optimize the speed of forest fire. Firstly, the Rothermel formula of fire speed is simplified, and the speed value of simplified Rothermel is optimized by the speed value of actual measured about fire spread, so that the optimal speed value is obtained, then the optimal speed is input into Cellular Automata (CA) to simulate the spread of forest fire. Secondly, the experiment is carried out by changing the slope, bed thickness, moisture content, load and wind speed, then the measured speed of fire spread, the speed of simplified Rothermel and the optimized speed by ENKF are compared in the process of fire spread. Finally, the experimental results show that the error of fire speed optimized by ENKF is smaller, the contour simulated by CA with the ENKF is closer to the contour of real fire spread, and the highest similarity index is 0.854. The model proposed in this paper has the ability to predict the spread of forest fire indoors.

Keywords: Ensemble Kalman filter; Rothermel forest fire spread formula; fire spread prediction; fire spread contour error

1 BACKGROUND

The forest fire is a serious natural disaster, which causes a lot of loss of people and property every year (Pagnini et al, 2014). Therefore, it is necessary to improve the existing model so that it can better predict the spread of forest fire (Dhall et al, 2017). At present, the forest fire spread models include the Rothermel of the United States, the MacArthur spread model of Canada, and the Wang Zhengfei model of China. The above are empirical models based on a large number of data. Currently, the models of forest fire spread obtained by scholars using intelligent algorithms are all based on the extension of the above models (Zhou et al, 2020). In recent years, with the great achievements of data assimilation in the weather forecasting, data assimilation methods have been widely used in other directions. For example, there are applications of data assimilation in the fields

of hydrological information, soil moisture, ocean surface information and so on (Metref et al, 2019).

Ntinis (2016) proposed the Fuzzy CA (FCA) model adopted a data-driven approach based on evolutionary optimization, which allowed incorporating knowledge from real wildfire in order to enhance its accuracy, then the model is compared with two different models of forest fire spread and the observed forest fire in the paper, the results shown that the model proposed in the paper had a strong practicality. Denham (2012) described a Dynamic Data-Driven Genetic Algorithm (DDDGA) used as steering strategy to automatically adjust highly dynamic input data values of forest fire simulators taking into account the underlying propagation model and real fire behaviour, the experimental results shown that the prediction method of forest fire spread proposed in this paper was an important improvement compared with

the previous algorithms. Valero (2017) used unsupervised edge detectors to automatically track the location around the fire, the remote sensing data were used to optimize the fuel and wind parameters of the simulator, which were assumed to remain unchanged for a certain period of time, and the optimal parameters were used to predict the fire development, the experiments showed that it can be adapted to sufficiently complex and diverse data sets.

There is a great advantage about the algorithm proposed by scholars, but it is necessary to analyze and store the covariance matrix with time in the process of calculating fire spread, which will increase the running time of the algorithm. In addition, many scholars use computer software to verify the model instead of carrying out real fire spread experiments, and fail to fully consider the complex influencing factors such as wind speed and moisture content in fire spread. In this paper, the prediction model of forest fire spread is established by using CA and data assimilation method. The simulated speed of the simplified Rothermel is optimizing by the observed speed with the data assimilation, then the optimal speed of the forest fire spread is obtained. The simulated contour of fire spread is obtained by combining the optimal speed with the CA, and the accuracy of the model is verified by the combustion experiment in the laboratory, which provides a new idea for the forest fire spread prediction model.

2 METHODS

As a bridge between observed data and simulated data, the method of data assimilation has been concerned by scholars. At present, the data assimilation has been widely used in many fields, such as atmosphere, ocean, ecology and so on (Pilo et al, 2018). The data assimilation (Jin et al, 2018) is on the basis of model dynamics, combining direct or indirect observed data, integrating the model and various observed factors at the same time, and constantly relying on the observed data to adjust the model to reduce errors. The data assimilation includes four basic elements (Tartes et al, 2014), and the corresponding four elements applied in the field of fire spread are: model of fire spread, observed data of fire spread, data assimilation algorithm, basic parameters. As a kind of data assimilation, Ensemble Kalman Filter (ENKF) algorithm overcomes the weakness that Kalman Filter requires tangent model, it also solves the problem of the amount of calculation of Kalman Filter algorithm in calculating the covariance of prediction error. For data assimilation of fire spread, it is obvious that ENKF is more advantages (Reichle et al, 2002).

The model of fire spread optimized by ENKF is a combination of observed and simulated data to achieve predicted speed of fire in short time. The simulated value of the model and the observed value of the real fire spread are needed in the algorithm, so it is necessary to select the appropriate fire spread model to realize the accurate prediction of the fire contour. In this paper, The fire speed of the simplified Rothermel is the simulated value, The fire speed recorded by the camera and calculated by image processing is the observed value. The matrix transformation is used to transform the image coordinates of fire contour into world coordinates as the observed data of the fire spread. The technical scheme of this paper is shown in the Fig. (1).

2.1 Simplified model of the Rothermel speed

The Rothermel is a common forest fire spread speed model, which is an empirical model based on a large number of data. As shown in Eq. (1), it is the Rothermel formula of forest fire spread speed:

$$R = \frac{I_R \times \zeta \times (1 + \Phi_W + \Phi_S)}{P_b \times \varepsilon \times Q_{ig}} \quad (1)$$

where, the I_R is the reaction intensity, the ζ is the spreading rate, the Φ_W is the wind speed correction coefficient, the Φ_S is slope correction coefficient, the P_b is the drying particle density, the ε is the effective heat coefficient, and the Q_{ig} is the precombustion heat. The model needs to input a lot of parameters, and there is a nested relationship between the parameters, so it needs to be simplified. The simplified formula is shown in Eq. (2).

$$R = B\delta \left(K \frac{W_0}{\delta}\right)^C \exp\left[C \cdot \left(1 - K \frac{W_0}{\delta}\right) + E\left(K \frac{W_0}{\delta} + 0.1\right)f(m)\right] \left[1 + GU^H \left(K \frac{W_0}{\delta}\right)I + J\left(\frac{W_0}{\delta}\right)^{-0.3}(\tan\Phi)^2\right] \quad (2)$$

where B , C , E , G , H , I , J and K are the parameters to be estimated respectively, and the methods have been given in the previous studies (Hua et al, 2020). The δ is the thickness of combustible bed, the W_0 is the load of dried combustibles, the U is the wind speed in the middle of the flame, the Φ is the slope angle, the M_f is the moisture content of combustibles, the M_x is the extinguishing moisture content of combustibles, the $f(m)$ is a function containing M_f and M_x . The U , W_0 , Φ , $f(m)$ and δ are independent variables, and the R is the speed of forest fire which is a dependent variable in the Eq. (2).

2.2 Observed speed value of forest fire spread

In order to find the speed of fire spread, the pixel coordinates of the fire contour in the image must be

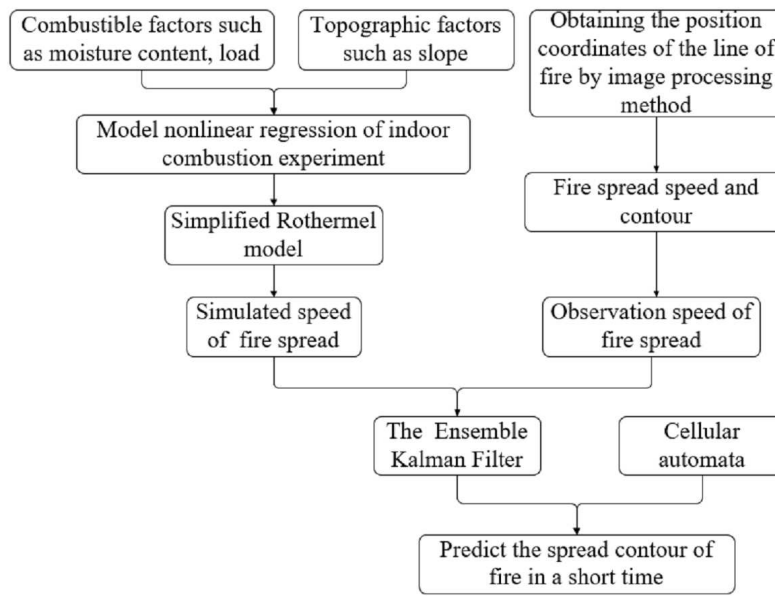


Figure 1: The technical scheme of this paper.

transformed into the coordinates in the world coordinate system. According to the principle of Perspective Transformation (Rossi et al, 2019), the coordinates of point pixels in an image is to transform the coordinates of the real corresponding points, and the speed of the fire spread is obtained. As shown in the Eq. (3), it is the Perspective Transformation.

$$\begin{bmatrix} X \\ Y \\ Z \end{bmatrix} = \begin{bmatrix} a_{11} & a_{12} & a_{13} \\ a_{21} & a_{22} & a_{23} \\ a_{31} & a_{32} & a_{33} \end{bmatrix} \begin{bmatrix} x \\ y \\ 1 \end{bmatrix} \quad (3)$$

where $\begin{bmatrix} a_{11} & a_{12} & a_{13} \\ a_{21} & a_{22} & a_{23} \\ a_{31} & a_{32} & a_{33} \end{bmatrix}$ is the Perspective transformation matrix,

$\begin{bmatrix} x \\ y \\ 1 \end{bmatrix}$ is pixel coordinates in an image, $\begin{bmatrix} X \\ Y \\ Z \end{bmatrix}$

is real coordinates of the corresponding point. Since all the points are in the same plane, Eq. (4) and Eq. (5) can be obtained by dividing both sides of the equation in Eq. (3) by Z at the same time:

$$\begin{cases} X' = \frac{X}{Z} \\ Y' = \frac{Y}{Z} \\ Z' = \frac{Z}{Z} \end{cases} \quad (4)$$

simplify:

$$\begin{cases} X' = \frac{a_{11}x+a_{12}y+a_{13}}{a_{31}x+a_{32}y+a_{33}} \\ Y' = \frac{a_{21}x+a_{22}y+a_{23}}{a_{31}x+a_{32}y+a_{33}} \\ Z' = 1 \end{cases} \quad (5)$$

The $\{a_{11}, a_{12}, a_{13}, a_{21}, a_{22}, a_{23}, a_{31}, a_{32}\}$ can be solved by finding four known coordinates in the image accord-

ing to Eq. (5). The camera can easily identify the corners of the four corners of the calibration plate, so it is necessary to put the calibration plate on the combustion bed before the experiment, and the coordinates of all the points on the combustion plane can be obtained through the calibration plate. As shown in the Fig. (2), the calibration plate is placed on the combustion bed.



Figure 2: The position of calibration plate and combustion bed.

When the coordinates of the points on the fire contour are known, the ratio of the distance between the two fire contours to the interval time is the spread speed of the fire. As shown in Fig. (3), it is the calculation for speed of fire contour. At the initial time, the point P_1 is selected on the fire line of “L”, make the tangent of the fire line of “L” through P_1 , and then make the perpendicular line of the tangent line after P_1 , and the intersection P'_1 of this vertical line and the next time of fire line “L” is the corresponding spreading point of the next time.

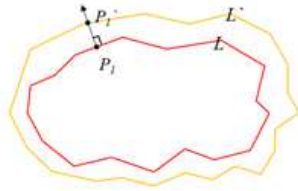


Figure 3: The schematic of fire line speed calculation.

2.3 Prediction model of forest fire spread based on ENKF

The basic method of ENKF (Rochoux et al, 2014) algorithm is to assume a set for the state quantity, each set represents the possible value of the state quantity, and the mean value of the set is the optimal estimation of the state quantity. Each set is integrated forward through the model to predict the amount of state of each set at the next time. For each moment when there is observed data, each set is updated separately with the observed data. In this case, the mean value of all sets is the optimal estimated value of the state quantity.

(1) State Vector

In order to assimilate the predicted speed of fire spread by ENKF, it is necessary to generate the state vector of the initial set. The state vector is shown in Eq. (6):

$$y_{t,j} = \{R\}, j = 1 \dots \dots N \quad (6)$$

where the $y_{t,j}$ is the State Vector, the t is the time, the j is the member of the set, the N is the number of the set, the R is the speed of the fire.

(2) Prediction process

The predicted state vector of the current moment can be obtained from the analysis of the previous moment by Eq. (7), in the predicted step, all the dynamic parameters change with time.

$$y_{t,j}^f = F(y_{t-1,j}^a) \quad (7)$$

where the $F(\cdot)$ is the model of fire spread speed, the f is the predicted value, the a is the analytical value. The $y_{t,j}^f$ is the forecast state vector of set member j at time t , and $y_{t-1,j}^a$ is the analytical value state vector of and set member j at time t .

(3) Generate disturbance observations

In the update phase, it is necessary to disturb the observed data to get the observed vectors of each set member at the time t .

$$d_{t,j}^{uc} = y_t^O - Hy_{t,j}^f + v(n) \quad (8)$$

where the $d_{t,j}^{uc}$ is the disturbance data of j set at time t of fire spread, the y_t^O is the observed speed of time t , the H is the observed factor and the mapping from state

variables to observed data, the $v(n)$ is an observed error and satisfies that the mean value is 0 and the covariance matrix is R_t normal distribution.

(4) Data assimilation

$$y_{t,j}^a = y_{t,j}^f + K_t d_{t,j}^{uc} \quad (9)$$

where the $y_{t,j}^a$ is the analytical value of j set at t time, the K_t is the set Kalman filter factor, and the K_t is composed of observed error variance matrix R_t , variance matrix of state predicted error P_t^f and observed factor H .

$$K_t = P_t^f H^T (HP_t^f H^T + R_t)^{-1} \quad (10)$$

where

$$P_t^f = \frac{1}{N-1} \sum_{j=1}^N (y_{t,j}^f - \bar{y}_{t,j}^f)(y_{t,j}^f - \bar{y}_{t,j}^f)^T \quad (11)$$

The analytical value of model by data assimilation at the current time and the predicted value of the model at the next time can be obtained by Eq. (7)-Eq. (9). As shown in the Fig. (4), it is the process of predicting fire spread by the ENKF.

2.4 Forest Fire Spreading Model of CA

The self-organization of Cellular Automata (CA) is similar the fire spread (Hui et al, 2016). It is a new method to combine empirical model with CA to form a new semi-physical and semi-empirical model of forest fire spread (Sun et al, 2013). In this paper, the method of combining Rothermel with CA can well simulate the spread of forest fire, so as to realize the simulation of forest fire spread. The CA is composed of cellular space, cellular domain, cellular state and local transition rules. In this paper, the space of the defined cell is consistent with the size of the actual burning area, and eight domains are selected as the domain of the cell. Next, the cellular state and local transition rules of CA will be introduced in detail.

(1) The Cellular state

As shown in the Eq. (13), the state value can be determined according to the ratio of the burning area to the cell area, and the state value can be divided into three types: state 1 ($A_{i,j}^t = 0$) is combustible, but has not been ignited, state 2 ($0 < A_{i,j}^t < 1$) is burning and not fully burned, and state 3 ($A_{i,j}^t = 1$) is that the fuel has been burned, which can't be ignited and burned. If the state of the cell is 1, the next moment is state 2. If the state of the cell is 2, the state of the cell at the next moment is 3, which means that the existing fuel has been burnt out and can no longer be ignited and burned.

$$A_{ij}^t = \frac{S_{BurningArea}}{S_{Cellarea}} \quad (12)$$

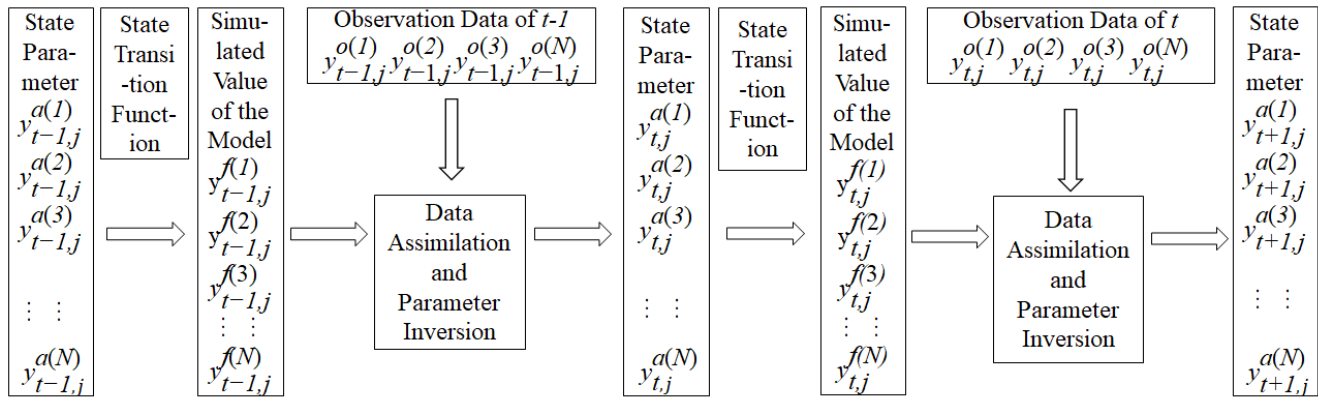


Figure 4: The ENKF forest fire spread prediction model.

(2)The local transition rules of CA

As shown in Eq. (13) and Fig. (5), the burning state of the central cell at the $t + \Delta t$ is determined by the state of the domain cell at the time t and the spreading speed of the domain cell.

$$A_{i,j}^{t+\Delta t} = A_{i,j}^t + f(R_{1 \rightarrow 5}^t, R_{1 \rightarrow 5}^t, R_{2 \rightarrow 5}^t, R_{3 \rightarrow 5}^t, R_{4 \rightarrow 5}^t, R_{6 \rightarrow 5}^t, R_{7 \rightarrow 5}^t, R_{8 \rightarrow 5}^t, R_{9 \rightarrow 5}^t) \quad (13)$$

where the R is the speed of fire spread, and its value is calculated by the simplified Rothermel.

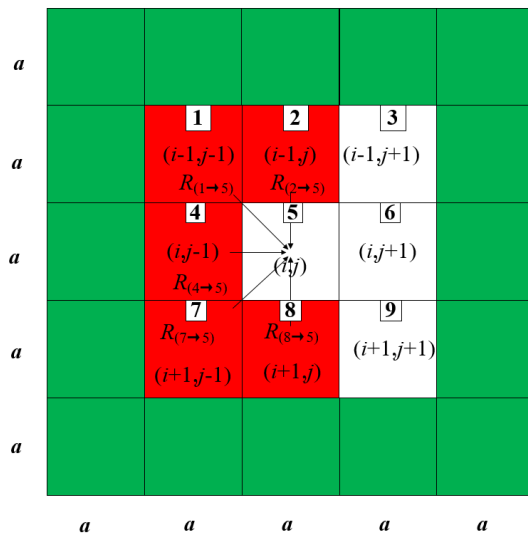


Figure 5: The state of CA.

The state of the central cell at the time $t + \Delta t$ can be calculated by the Eq. (14). As shown in Eq. (14) and Fig. (6), the eight cells around the central cell are divided into 2, 4, 6, 8 domain cells and 1, 3, 7, 9 sub-domain cells. The position of domain cells and sub-domain cells

relative to the central cell is different, so the local transition rules need to be discussed separately. Firstly, for the 2, 4, 6, 8 domain cells, take the cell $2(i - 1, j)$ as an example, the speed of cell $2(i - 1, j)$ spreading to cell $5(i, j)$ is $R_{(2 \rightarrow 5)}$, the time is Δt , the side length of the cell is a , the burning area of the cell $S = a \cdot R_{(2 \rightarrow 5)} \cdot \Delta t$ can be calculated, and then the burning area ratio is $\frac{R_{(2 \rightarrow 5)} \cdot \Delta t}{a}$. Similarly, the burning area and burning area ratio of the cells in the other three domains 4, 6, 8 can be obtained. Secondly, for the 1, 3, 7, 9 sub-domain cells, take the cell $7(i - 1, j - 1)$ as an example, the speed of cell $7(i - 1, j - 1)$ spreading to cell $5(i, j)$ is $R_{(7 \rightarrow 5)}$, the time is Δt , the side length of the cell is a , the burning area of the cell $S = \frac{(R_{(7 \rightarrow 5)} \Delta t)^2}{2}$ can be calculated, and then the burning area ratio is $\frac{(R_{(7 \rightarrow 5)} \Delta t)^2}{2a^2}$. Similarly, the burning area and burning area ratio of the cells in the other three sub-domains 1, 3, 9 can be obtained. It is concluded that the local transition rules of domain cell $1(i - 1, j - 1)$, $3(i - 1, j + 1)$, $7(i + 1, j)$, $9(i + 1, j + 1)$, $2(i - 1, j)$, $4(i, j - 1)$, $6(i, j + 1)$, $8(i + 1, j)$ around central cell $5(i, j)$ are obtained:

$$A_{i,j}^{t+\Delta t} = A_{i,j}^t + \frac{(R_{2 \rightarrow 5}^t + R_{4 \rightarrow 5}^t + R_{6 \rightarrow 5}^t + R_{8 \rightarrow 5}^t) \Delta t}{a} + \frac{[(R_{1 \rightarrow 5}^t)^2 + (R_{3 \rightarrow 5}^t)^2 + (R_{7 \rightarrow 5}^t)^2 + (R_{9 \rightarrow 5}^t)^2] \Delta t^2}{2a^2} \quad (14)$$

where $A_{i,j}^{t+\Delta t}$ is the cellular state of the cell at the t time. Only when the state value of the cell is ≥ 1 , the cell is completely burned, and the cell has the ability to spread to the surrounding eight cells, otherwise the cell does not have the ability to spread. Where the Δt is 1 second, the a is the side length of a single cell, according to the total numbers of the cells and the total areas of the combustion bed, it is concluded that the side length

of a single treasure is 0.02m, and R is the speed of fire spread in eight directions.

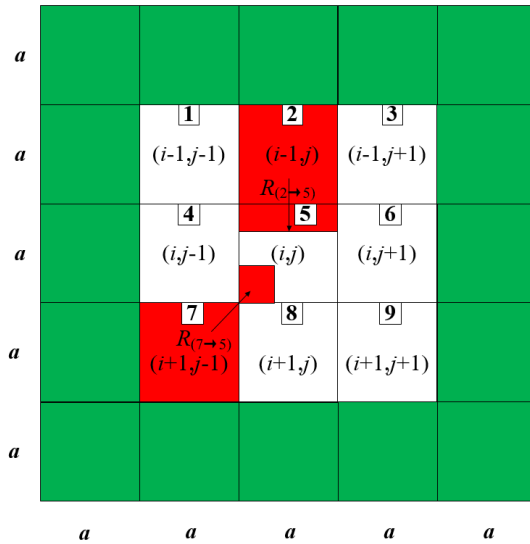


Figure 6: The speed of CA.

3 EXPERIMENTS AND RESULTS

The place of experiment is the Maoershan Forest Fire Research Laboratory($N45^\circ, E127^\circ$) of Northeast Forestry University, and the details of the experiment are as follows. The inclination of the combustion bed are 0° and 8° , the speed of wind is recorded by the anemometer, and the area of combustible material is $0.8m \times 0.6m$. The spread of the fire is recorded by the camera, and the contour of the fire is obtained through the image processing technology. The *Pinussylvestris* var. *mongolica* is taken as the research object of this paper, because of the large quantity and strong flammability in Maoershan. The experiment dataset consists of the training datasets and testing datasets in the paper. In the training datasets, the angles between the direction of fire spread and the direction of wind are $0^\circ, 45^\circ, 90^\circ, 135^\circ$ and 180° , which are the 8 directions of CA. The aim of the training dataset is to obtain the value of the B, C, E, G, H, I, J and K after knowing the dependent variable and independent variable in the simplified Rothermel formula. Through the training datasets, the speeds of simplified Rothermel in eight directions are obtained. In the testing datasets, the slope of the combustion bed are two stages to verify the accuracy of the model in the same fire spread. The training datasets and the testing datasets are shown in the Tab. 1 and Tab. 2.

The parameters B, C, E, G, H, I, J and K of simplified Rothermel in eight directions are obtained by non-linear fitting using LM (Levenberg-Marquardt) method, that is, the speeds of the local transition rules in CA are obtained, the contour of the fire spread is simulated by CA. For simplicity, the speed in the direction of the fire front is used as the object of comparison, the speed optimized by the ENKF and the speed of simplified Rothermel are compared. The speed variation with time about the testing datasets are shown in Fig. (7) and Fig. (8). As shown in Fig. (7) and Fig. (8), the blue broken line is the speed optimized by ENKF, the red one is the speed simulated by the simplified Rothermel, and the black one is the measured value. The error bar is also shown in the blue and red broken lines in the figures. It can be seen from the figures that the speed optimized by the ENKF is closer to the measured value, and the error is smaller.

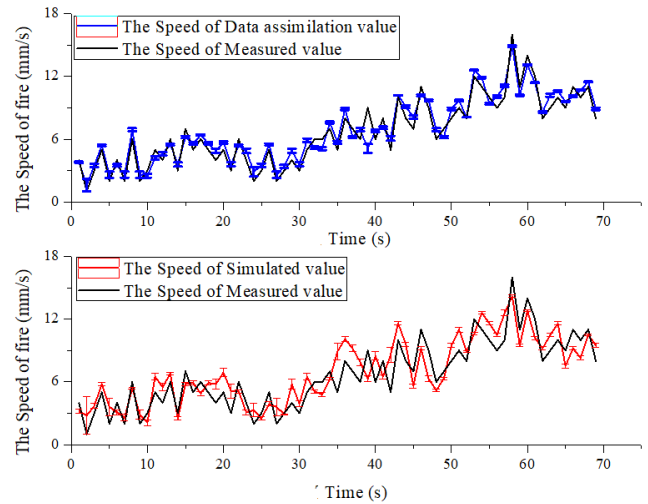


Figure 7: The speed of fire spread and the error bar with time about the testing dataset 1.

The real contour of fire spread is obtained by using the method of image processing. The last moment contour of fire spread is shown in the Fig. (9) and Fig. (10). The black line is the real contour of fire spread, the red one is the contour simulated by CA with the simplified Rothermel, and the blue one is contour simulated by CA with the optimized by the ENKF. Eq. (15) is the formula for measuring contour similarity (Finney et al, 2013), the closer the contour similarity is, the closer the value of J is to 1.

$$J = \frac{A^{ob} \cap A^m}{A^{ob} \cup A^m} \quad (15)$$

where the A^{ob} is the value of the observed area, the A^m is the area value simulated for the model.

Table 1: The training datasets.

| No. | Weight (kg) | Aera (m ²) | Load (kg/m ²) | Thickness (m) | Slope (°) | Moisture content (%) | Angle between wind direction and spread direction(°) |
|-----|-------------|------------------------|---------------------------|---------------|-----------|----------------------|--|
| 1 | 0.69 | 0.8*0.6 | 1.44 | 0.05 | Up/8 | 5.24% | 0 |
| 2 | 0.62 | 0.8*0.6 | 1.29 | 0.04 | Up/8 | 6.14% | 45 |
| 3 | 0.83 | 0.8*0.6 | 1.73 | 0.07 | Up/8 | 7.00% | 90 |
| 4 | 0.91 | 0.8*0.6 | 1.9 | 0.07 | Up/8 | 8.37% | 135 |
| 5 | 0.63 | 0.8*0.6 | 1.31 | 0.06 | Up/8 | 8.37% | 180 |
| 6 | 0.93 | 0.8*0.6 | 1.93 | 0.07 | Down/8 | 8.92% | 0 |
| 7 | 0.53 | 0.8*0.6 | 1.1 | 0.05 | Down/8 | 8.92% | 45 |
| 8 | 0.55 | 0.8*0.6 | 1.14 | 0.05 | Down/8 | 8.81% | 90 |
| 9 | 1.09 | 0.8*0.6 | 2.26 | 0.08 | Down/8 | 6.49% | 135 |
| 10 | 0.73 | 0.8*0.6 | 1.52 | 0.05 | Down/8 | 8.81% | 180 |
| 11 | 1.01 | 0.8*0.6 | 2.1 | 0.08 | Flat/0 | 5.24% | 0 |
| 12 | 0.79 | 0.8*0.6 | 1.65 | 0.04 | Flat/0 | 6.14% | 45 |
| 13 | 0.92 | 0.8*0.6 | 1.92 | 0.07 | Flat/0 | 6.45% | 90 |
| 14 | 0.8 | 0.8*0.6 | 1.67 | 0.05 | Flat/0 | 5.10% | 135 |
| 15 | 0.98 | 0.8*0.6 | 2.05 | 0.07 | Flat/0 | 5.10% | 180 |

Table 2: The testing datasets.

| No. | Slope(°) | Wind direction | Area of first stage(m ²) | Area of second stage (m ²) | Load (kg/m ²) | Thickness (m) | Moisture content |
|-----|---------------|----------------|--------------------------------------|--|---------------------------|---------------|------------------|
| 1 | Flat-Up/8° | Downwind | 0.8*0.5 | 0.8*0.5 | 2.28 | 0.05 | 7.68% |
| 2 | Up/8°-Down 8° | Headwind | 0.8*0.5 | 08.*0.5 | 1.82 | 0.05 | 5.38% |

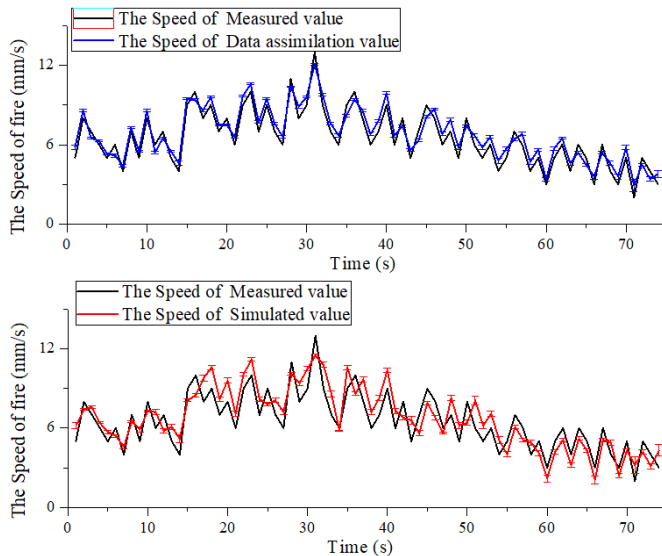


Figure 8: The speed of fire spread and the error bar with time about the tesing dataset 2.

The similarity index J for last moment of fire spread are shown as follows. For testing dataset 1, the similarity

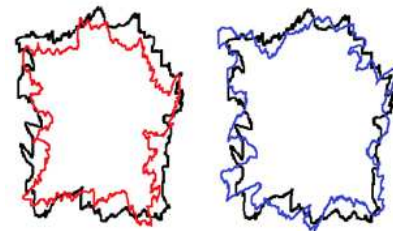


Figure 9: The contour comparison about the testing dataset 1.

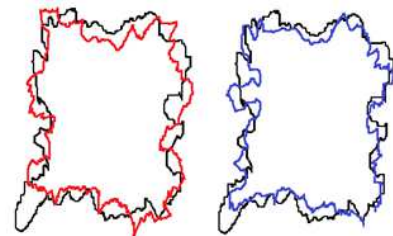


Figure 10: The contour comparison about the tesing dataset 2.

index J of contour simulated by CA with the simplified Rothermel and real contour is 0.782, the similarity index J of contour simulated by CA with the ENKF and real contour is 0.854. For testing dataset 2, the similarity index J of contour simulated by CA with the simplified Rothermel and real contour is 0.755, the similarity index J of contour simulated by CA with the ENKF and real contour is 0.838. It can be seen that the similarity index J of contour simulated by CA with the ENKF is close to 1, that is, the model simulation by ENKF is better.

4 CONCLUSION

It is found that the existing model fails to take into account the influence of many factors on the spread of forest fire, so the simulated speed of the model is quite different from the spread of real speed, and this error will increase with the increase of time. In this paper, a optimized algorithm of fire speed based on ENKF is proposed. To achieve the purpose of eliminating errors through the ENKF, the simulated speed of the simplified Rothermel is combined with the the real measured speed, and the contour of forest fire spread is simulated by CA with the ENKF. The experimental results show that the contour simulated by CA with the ENKF has a better effect.

The experimental results show that the model proposed in this paper has a good prediction effect, however there are still errors. The main reason for the error is that the moisture content of combustible materials changes with time. In the future research, more combustibles and larger burning area should be used to verify the effectiveness of the model.

ACKNOWLEDGEMENT

This work is supported by “Natural Science Foundation of Heilongjiang Province of China (Grant No. TD2020C001)”; “Fundamental Research Funds for the Central Universities (Grant No.2572019CP20)”.

REFERENCES

- Dhall, A., Dhasade, A., Nalwade, A., et al. 2020. A survey on systematic approaches in managing forest fires. *Applied Geography*, 121:102266. DOI:10.1016/j.apgeog.2020.102266.
- Denham, M., Wendt, K., Bianchini, G., et al. 2012. Dynamic Data-Driven Genetic Algorithm for forest fire spread prediction. *Journal of Computational Science*, 3(5):398-404. DOI:10.1016/j.jocs.2012.06.002.

Finney, M.A., Grenfell, I.C., Mchugh, C.W., et al. 2011. A method for ensemble wildland fire simulation. *ENVIRONMENTAL MODELING AND ASSESSMENT*, 16(2):153-167. DOI:10.1007/s10666-010-9241-3.

Finney, M., Cohen, J., McAllister, S., Jolly, W. 2013. On the need for a theory of wildland fire spread. *International Journal of Wildland Fire*, 22(1):25–36. DOI:10.1071/WF11117.

Hua, J., Zhang, S., Gao, H., et al. 2020. Optimizing the Rothermel model for easily Predicting spread rate of forest fire. *Mathematical and Computational Forestry and Natural-Resource Sciences*, 12(2):62-71.

Hui, S., Rui, X., Li, Y., et al. 2016. An Improved Forest Fire Spread Simulation Algorithm Coupled with Cellular Automata. *Geomatics and information Science of Wuhan University*, 41(10):1326-1332. DOI:10.13203/j.whugis20140811.

Jin, X., Kumar, L., Li, Z., et al. 2018. A review of data assimilation of remote sensing and crop models. *European Journal of Agronomy*, 92:141-152. DOI:10.1016/j.eja.2017.11.002.

Metref, S., Hannart, A., Ruiz, J., et al. 2019. Estimating model evidence using ensemble-based data assimilation with localization - the model selection problem. *Quarterly Journal of the Royal Meteorological Society*, 145:1571-1588. DOI:10.1002/qj.3513.

Ntinias, V., Moutafis, B., Trunfio, G., et al. 2016. Parallel Fuzzy Cellular Automata for Data-Driven Simulation of Wildfire Spreading. *Journal of Computational Science*, 21(7):469-485. DOI:10.1016/j.jocs.2016.08.003.

Pagnini, G., Mentrelli, A.. 2014. Modelling wildland fire propagation by tracking random fronts. *Natural Hazards and Earth System Sciences*, 14(6):6521-6557. DOI:10.5194/nhess-14-2249-2014.

Pilo, G., Oke, P., Richard, C., et al. 2018. Impact of data assimilation on vertical velocities in an eddy resolving ocean model. *Ocean Modelling*, 131:71-85. DOI:10.1016/j.ocemod.2018.09.003.

Rossi, L., Molinier, T., Akhloufi, M.. 2019. Advanced stereovision system for fire spreading study. *Fire Safety Journal*. 60(8):64-72. DOI:10.1016/j.firesaf.2012.10.015.

Reichle, R., Walker, J., Koster, R.D., et al. 2002. Extended versus Ensemble Kalman filtering for land data assimilation. *Hydrometeorol*, 3:728-740. DOI:10.1175/1525-7541(2002)0032.0.CO;2.

Rochoux, M., Emery, C., Ricci, S., et al. 2014. Towards predictive data-driven simulations of wildfire spread - Part II: Ensemble Kalman Filter for the state estimation of a front-tracking simulator of wildfire spread. *Natural Hazards and Earth System Sciences Discussions*, 2(5):3769-3820. DOI:10.5194/nhess-15-1721-2015.

Sun, T., Zhang, L., Chen, W., et al. 2013. Mountains forest fire spread simulator based on geo-cellular automaton combined with wang zhengfei velocity model. *IEEE Journal of Selected Topics in Applied Earth Observations and Remote Sensing*, 6(4):1971-1987. DOI:10.1109/JSTARS.2012.2231956.

Tartes, A., Cortes, Margalef. 2014. Towards a dynamic data driven wildfire behavior prediction system at european level. *Procedia Computer Science*, 29:1216-1226. DOI:10.1016/j.procs.2014.05.109.

Valero, M., Rios, O., Mata, C., et al. 2017. An integrated approach for tactical monitoring and data-driven spread forecasting of wildfires. *Fire Safety Journal*, 91(7):835-844. DOI:10.1016/j.firesaf.2017.03.085.

Zhou, T., Ding, L., Ji J., et al. 2020. Combined estimation of fire perimeters and fuel adjustment factors in farsite for forecasting wildland fire propagation. *Fire Safety Journal*, 116(9):103167. DOI:10.1016/j.firesaf.2020.103167.